A Path Generation Algorithm of an Automatic Guided Vehicle Using Sensor Scanning Method

Tong-Jin Park, Jung-Woo Ahn
Research assistant, Department of Precision Mechanical Engineering, Hanyang University, Kyunggi-do 425-791, Korea
Chang-Soo Han*
Professor, Department of Mechanical Engineering, Hanyang University, Kyunggi-do 425-791, Korea

In this paper, a path generation algorithm that uses sensor scannings is described. A scanning algorithm for recognizing the ambient environment of the Automatic Guided Vehicle (AGV) that uses the information from the sensor platform is proposed. An algorithm for computing the real path and obstacle length is developed by using a scanning method that controls rotating of the sensors on the platform. The AGV can recognize the given path by adopting this algorithm. As the AGV with two-wheel drive constitute a nonholonomic system, a linearized kinematic model is applied to the AGV motor control. An optimal controller is designed for tracking the reference path which is generated by recognizing the path pattern. Based on experimental results, the proposed algorithm that uses scanning with a sensor platform employing only a small number of sensors and a low cost controller for the AGV is shown to be adequate for path generation.

Key Words: AGV (Automatic Guided Vehicle), Scanning Method, Sensor Platform, Path Recognition, Path Tracking, Path Generation

Nomenclature

F_0 : Global frame
F_M : AGV's frame
r : Radius of actuated wheel [m]
R : Half the wheels' axis length [m]
v : AGV's translation velocity [m/s]
x, y : Coordinates of the F_M
x_p, y_p : Coordinates of the point F_0
x_M, y_M: Coordinates of the point F_0
θ_1 : Angular position of the right wheel [rad]
θ_2 : Angular position of the left wheel [rad]
Ψ : AGV's orientation with respect to the F_0
d : Length from the AGV to an object [m]

Subscripts

s : Sensor coordinate
ob/M: Coordinate of an object about the AGV
M : The AGV Coordinate

* Corresponding Author,
E-mail : cshan@hanyang.ac.kr
TEL : +82-31-400-5247; **FAX** : +82-31-406-6242
Professor, Department of Mechanical Engineering, Hanyang University, Kyunggi-do 425-791, Korea.
(Manuscript **Received** July 25, 2000; **Revised** November 19, 2001)

1. Introduction

The AGV should generate a proper path for obstacle avoidance, path recognition, and path for reaching a goal point. Thus any study for the path generation algorithm should contain path planning, obstacle avoidance, self-localization, and a self-organizing map.

Recent research works have been conducted with the aim of recogniting objects while reducing the number of sensors. Matthies and Shafer (1987) studied the path recognition problem by using a stereo camera. Miller and Wagner (1987) investigated the path generation algorithm that takes in the input of an infrared sensor using a rotating sensor platform. These papers have dealt with the issue of reducing the numbers of sensors,

with the algorithms focused on path recognition by using complicated hardware setups. After recognizing a path pattern or an object, the AGV constructs a path generation algorithm and then the AGV navigates by path tracking. A motor control is required for path tracking. A path tracking algorithm based on the feedback control of systems with the nonholonomic AGV kinematic model has been investigated (Samson and Ait-Abderrahim; 1991). Also Jang and Han (1997) devised a vehicle control scheme based on the vehicle modeling to enhance driving flexibility.

To perform path generation by one controller, the AGV should have a more effective sensing algorithm and an algorithm for motor control. In this paper, a path generation algorithm that uses the scanning method is described. For more effective use of the sensor input, actuators are designed into the sensor platform. For path tracking, an optimal controller based on a linearized kinematic AGV model is proposed. To apply the path generation algorithm, the sensor platform and the AGV are designed and experimented. The type of driving is two-wheel drive (2WD), in which the AGV is steered by taking the difference of the angular velocities of the two wheels.

2. Sensor platform

In this study, a sensor platform is designed to enhance the sensor inputs for more effective path recognition. The sensor platform serves to extend the sensor scope. An algorithm for recognizing objects is constructed from relationships between the sensor platform and the object. This section describes the design of the sensor platform for extending the sensor scope and modeling of sensor platform for recognizing objects.

2.1 Design of sensor platform

If the sensor inputs become larger, the sensor inputs require more accompanying filters or processing of large amounts of data. Consequently, better control is needed for the AGV to move at high speeds. Figure 1 shows the sensor platform that is operated by two electric motors.

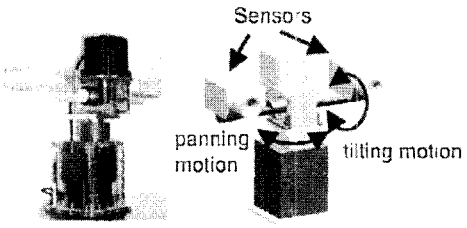

Fig. 1 Sensor platform

The sensor platform can be scanned by two electric motors with a transmission mechanism. To recognize the direction of the right and left path, the sensor platform utilizes a panning motion. To direct up and down movement, tilting motion is simultaneously available. It is composed of two sensor-decks with various sensors. In this paper, ultrasonic sensor is used. Ultrasonic range finders may have poor performance compared with optical range finders. In the previous research, a number of ultrasonic sensors were used. Ultrasonic sensor inputs are determined by the probability theory (Henderson; 1987, Flynn; 1988). However, using the sensor platform, the ultrasonic sensor is able to have a wide range by suitable filtering. Specifically, only the panning motion of the sensor platform is allowed to generate data for the algorithm governing the horizontal recognition of objects and their respective paths.

2.2 Scanning method

In this study, a scanning method algorithm is derived from the panning motion of the sensor platform. In the beginning, the AGV is assumed to be stationary. The sensor data are collected once in every sampling period. Each collected data set represent relative values obtained from the sensor frame on the AGV. Figure 2 represents the relative coordinates of the sensor and the object frame.

The mathematical formulae representing the object recognition measured in polar coordinates are as follows:

$$x_{ob/M}(k) = d(k)\cos\phi_s(k) \quad (1)$$

$$y_{ob/M}(k) = d(k)\sin\phi_s(k) \quad (2)$$

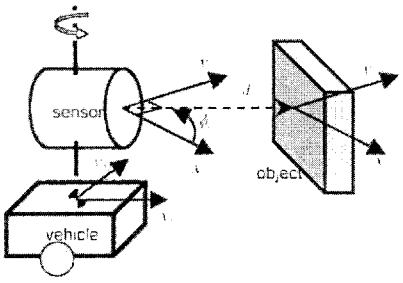

Fig. 2 Coordinates of the sensor and the object

where k denotes k-th sampling time, ϕ_s is the angle of the panning of the rotating sensor and d is the length from the AGV the an object. These formulae are converted to the absolute rectangular coordinates for representing any given object. The approximate shape of each object is modeled by linking the points indicated by their respective object coordinates. If Eq. (1) and Eq. (2) are applied to the moving AGV, the center position of the AGV is added to the scanning method algorithm. Related equations are as follows:

$$\begin{aligned} x_{ob}(k) &= x(k) + x_{obj\,m}(k) \\ &= x(k) + d(k)\cos\phi_s(k) \end{aligned} \tag{3}$$

$$\begin{aligned} y_{ob}(k) &= y(k) + y_{obj\,m}(k) \\ &= y(k) + d(k)\sin\phi_s(k) \end{aligned} \tag{4}$$

With sensor platform scanning, the size of the object is determined from Eq. (1) to Eq. (4). Several sensors were used for path recognition in the previous investigations (Henderson; 1987, Flynn; 1988). When using a scanning algorithm, path recognition is performed with one sensor.

3. Design of the AGV

A two-wheel drive AGV is developed and experiments are carried out on the sensor platform. Figure 3 shows the structure and design of the AGV.

The driving motor is composed of a body and a wheel. The driving motor and wheel sets are located at both sides. Two caster wheels are located at the front and rear of the AGV. The maximum speed of the motor is 0.075 m/sec and powered by a 24 V DC battery. The battery has 2 -hour continuous drive capacity at the maximum speed. This AGV was named 'HYAV1'.

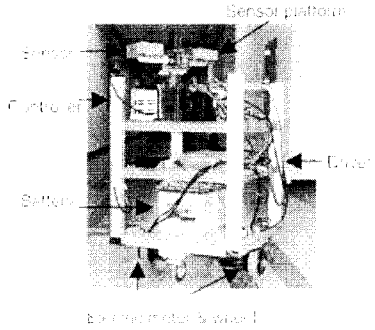

Fig. 3 The Automatic Guided Vehicle

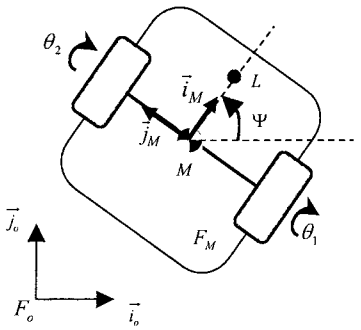

Fig. 4 Schematic diagram of AGV

As an object is measured by the sensor platform, the AGV is navigated based on the information gathered by the sensor and the user's prior instruction. Path generation is carried out by algorithm for path recognition and path tracking. As path tracking is completed by the motor control, a kinematic model of the AGV is required. This section describes the kinematic modeling and controller design for the AGV.

3.1 Modeling

Because of the nonholonomic constraint, the 2WD-AGV model considered here has only two-degree of freedom but three control variables (x, y, Ψ) as in the case for a two-steer vehicle (Yun and Nilanjan; 1996). The feedback linearization method is used for the 2WD-AGV which is steered by the velocity difference between two driving wheels.

Figure 4 shows the AGV model with two driving wheels. In order to obtain a simple kinematic model, it is assumed that no-slip condition exists between the wheels of the AGV and

the ground. Based on this assumption, the kinematic equations are as follows:

$$\dot{x}_M=\frac{r}{2}(\dot{\theta}_1+\dot{\theta}_2)\cos\Psi \tag{5}$$

$$\dot{y}_M=\frac{r}{2}(\dot{\theta}_1+\dot{\theta}_2)\sin\Psi \tag{6}$$

$$\dot{\theta}_M=\frac{r}{2}(\dot{\theta}_1-\dot{\theta}_2) \tag{7}$$

These formulae are general kinematic equations for a typical 2WD vehicle. However, there is a nonholonomic constraint that should be satisfied. The next equation expresses the nonholonomic constraint for the AGV.

$$\dot{x}_M\sin\Psi-\dot{y}_M\cos\Psi=0 \tag{8}$$

This constraint specifies the tangent direction along any feasible path for the robot and a bound on the curvature of the path. Notice that on the plane, the AGV motion possesses three degrees of freedom, steered by two control inputs and under the nonholonmic constraint (Lee, et. al; 1999, Park, et. al; 1999). Therefore, the control may not be easily achieved due to the presence of the nonholonomic constraint which cannot be precisely integrated with the center of the AGV body to produce a singular point.

A method that linearizes the singular point is thus employed in order to address this issue. A virtual point, L, which is linked to the AGV's frame, is located at distance l from the direction of wheel's axis of the AGV navigation. It can be expressed as.

$$\overrightarrow{ML}=l\cdot\vec{i}_M \tag{9}$$

The x, y coordinates of the vector with respect to the AGV's frame F_M can be expressed as

$$\overrightarrow{LO}=x\cdot\vec{i}_M+y\cdot\vec{j}_M \tag{10}$$

Eq. (11) and Eq. (12) represent the configuration and auxiliary vectors

$$\mathbf{x}=[x\ y\ \Psi]^T \tag{11}$$

$$\mathbf{u}=[v\ \dot{\Psi}]^T \tag{12}$$

In Eq. (12), v is the tangential velocity of the AGV along the $\vec{i}_M$ axis. The control vector $\mathbf{u}$ is constrained by the driving wheel velocity and represented by the following equations

$$\mathbf{u}=\begin{bmatrix}\frac{r}{2} & \frac{r}{2}\\ \frac{r}{2R} & -\frac{r}{2R}\end{bmatrix}\begin{bmatrix}\dot{\theta}_1\\ \dot{\theta}_2\end{bmatrix} \tag{13}$$

Therefore, the AGV's state equation is expressed by control input $\mathbf{u}$ as

$$\dot{\mathbf{x}}=\mathbf{A}(\mathbf{x})\cdot\mathbf{u} \tag{14}$$

To obtain matrix $\mathbf{A}(\mathbf{x})$, the relative velocity of any point $P(x_p, y_p)$ with respect to fixed frame F_o is described by

$$\vec{V}_{P/F_M}=\vec{V}_{P/F_O}-\vec{V}_{M/F_O}-\vec{w}_{F_M/F_O}\times\overrightarrow{MP} \tag{15}$$

Here, $\vec{w}_{F_M/F_O}$ is the instantaneous rotational velocity of the AGV's frame F_M with respect to the fixed frame F_o. In addition, $\vec{w}_{F_M/F_O}$ and $\overrightarrow{MP}$ are represented in the following equations

$$\vec{w}_{F_M/F_O}=\dot{\theta}\cdot\vec{k}_o \tag{16}$$

$$\overrightarrow{MP}=(l+x)\cdot\vec{i}_M+y\cdot\vec{j}_M \tag{17}$$

$$\vec{w}_{F_M/F_O}\times\overrightarrow{MP}=y\dot{\theta}\cdot\vec{i}_M-(l+x)\,\dot{\theta}\cdot\vec{j}_M \tag{18}$$

The velocity of point M with respect to the AGV's frame F_M is

$$\vec{V}_{M/F_o}=v\cdot\vec{i}_M \tag{19}$$

Therefore, Eq. (11) is transformed to the next equation by substituting Eq. (16) for Eq. (19)

$$\begin{bmatrix}\dot{x}\\ \dot{y}\end{bmatrix}=\begin{bmatrix}-1 & y\\ 0 & -(l+x)\end{bmatrix}\begin{bmatrix}v\\ \dot{\Psi}\end{bmatrix}+\begin{bmatrix}\cos\Psi & \sin\Psi\\ -\sin\Psi & \cos\Psi\end{bmatrix}\begin{bmatrix}\dot{x}_p\\ \dot{y}_p\end{bmatrix} \tag{20}$$

where the point P is the same as the origin of the fixed frame F_o, i.e., $\dot{x}_p=\dot{y}_p=0$. $\mathbf{A}$ matrix, $\mathbf{x}$ vector and $\mathbf{u}$ vector in Eq. (14) are expressed by the following equations

$$\mathbf{A}(\mathbf{x})=\begin{bmatrix}-1 & y\\ 0 & -(l+x)\\ 0 & 1\end{bmatrix} \tag{21}$$

$$\mathbf{x}=[x\ \ y\ \ \Psi]^T \tag{22}$$

$$\mathbf{u}=[v\ \ \dot{\Psi}]^T \tag{23}$$

Eqs. (21) ~ (22) show that the values of the open loop control depend on the initial position $\mathbf{x}$. However, this system is not controllable because matrix $\mathbf{A}$ is not square. This model should be considered as a RMFC (Reference Model Following Control) which is a path tracking algorithm.

3.2 Controller

Based on the linearized model, a controller is designed to track the reference path. An operational error occurs in the direction when the AGV deviates from the reference path. In this study, an optimal controller for minimizing this error is proposed.

Ψ_{A1} is the direction of the AGV when it is navigating by following the reference path and Ψ_{A2} is the direction when it is devistes from the path. The direction error between Ψ_{A1} and Ψ_{A2} is defined by

$$\tilde{\Psi}=\Psi_{A1}-\Psi_{A2} \tag{24}$$

The state vector is expressed as

$$\mathbf{x}=[x \quad y \quad \tilde{\Psi}]^T \tag{25}$$

$v(t)$ is the velocity of the AGV according to the desired path, the control input $\mathbf{u}$ becomes

$$\mathbf{u}=\begin{bmatrix}\tilde{v}\\ \dot{\tilde{\Psi}}\end{bmatrix}=\begin{bmatrix}v_{A2}-v_{A1}\\ \dot{\Psi}_{A2}-\dot{\Psi}_{A1}\end{bmatrix} \tag{26}$$

The system equation is

$$\dot{\mathbf{x}}=\mathbf{F}\mathbf{x}+\mathbf{G}\mathbf{u} \tag{27}$$

where,

$$\mathbf{F}=\begin{bmatrix}0 & \dot{\Psi}_{A1} & v_{A1}\dfrac{\cos\tilde{\Psi}-1}{\tilde{\Psi}}+l\cdot\dot{\Psi}_{A1}\dfrac{\sin\tilde{\Psi}}{\tilde{\Psi}}\\ \dot{\Psi}_{A1} & 0 & -v_{A1}\dfrac{\sin\tilde{\Psi}}{\tilde{\Psi}}+l\cdot\dot{\Psi}_{A1}\dfrac{\cos\tilde{\Psi}-1}{\tilde{\Psi}}\\ 0 & 0 & 0\end{bmatrix},$$

$$\mathbf{G}=\begin{bmatrix}-1 & y\\ 0 & -(l+x)\\ 0 & 1\end{bmatrix}$$

The optimal control which chooses the control input, with which the AGV can track the reference path, involves the quadratic optimal control method. The performance index selected is

$$J=\int_0^{+\infty}(\mathbf{X}^T\mathbf{Q}\mathbf{X}+\mathbf{U}^T\mathbf{R}\mathbf{U})\,dt \tag{28}$$

The linear control input minimizing the performance index is as follows

$$\mathbf{U}=\mathbf{K}\mathbf{X} \tag{29}$$

where $\mathbf{K}=-\mathbf{R}^{-1}\mathbf{G}^T\mathbf{P}$

In Eq. (29), matrix $\mathbf{P}$ can be found by solving the following Riccati equation:

$$(\mathbf{F}-\mathbf{K}\mathbf{G})^T\mathbf{P}+\mathbf{P}(\mathbf{F}-\mathbf{K}\mathbf{G})+\mathbf{Q}+\mathbf{K}^T\mathbf{R}\mathbf{K}=0 \tag{30}$$

where

$$\mathbf{F}=\begin{bmatrix}0 & 0 & 0\\ 0 & 0 & -v_{A1}\\ 0 & 0 & 0\end{bmatrix},\quad \mathbf{G}=\begin{bmatrix}-1 & 0\\ 0 & 0\\ 0 & 1\end{bmatrix},$$

$$\mathbf{P}=\begin{bmatrix}1 & 0 & 0\\ 0 & \dfrac{\sqrt{1+2|v_{A1}|}}{|v_{A1}|} & -sign(v_{A1})\\ 0 & -sign(v_{A1}) & \sqrt{1+2|v_{A1}|}\end{bmatrix}$$

By substituting matrix P in Eq. (30), the control gain matrix K can be obtained

$$\mathbf{K}=\begin{bmatrix}1 & 0 & 0\\ 0 & sign(v_{A1}) & -\sqrt{1+2|v_{A1}|}\end{bmatrix} \tag{31}$$

As pointed out in section 3.1, the system is not controllable when the AGV is motionless ($v_{A1}=\dot{\Psi}_{A1}=0$) on the reference path. However, the system becomes controllable as soon as the AGV starts moving. By using the control gain matrix $\mathbf{K}$, the path tracking algorithm is constructed.

3.3 Path generation algorithm

The AGV initially navigates by following the recognized path pattern as set by the user input. If the AGV encounters an obstacle, it needs to avoid it. When deviating from the path to avoid an obstacle, it should track the path which was recognized initially as the path pattern. In this study, the optimal controller is used for path tracking.

The path generation algorithm for navigating consists of two parts: recognized path navigation and path tracking navigation. Path recognition is the algorithm for navigating the AGV along the path. It is the recognition of the navigating path pattern which is designed as the reference path. Path tracking is the algorithm for tracking the reference path when obstacles are encountered. The flow chart of the path generation algorithm is shown in Fig. 5.

4. Simulations

Path recognition is verified by the scanning method based on the modeling of the sensor platform. Path tracking is achieved by the optimal

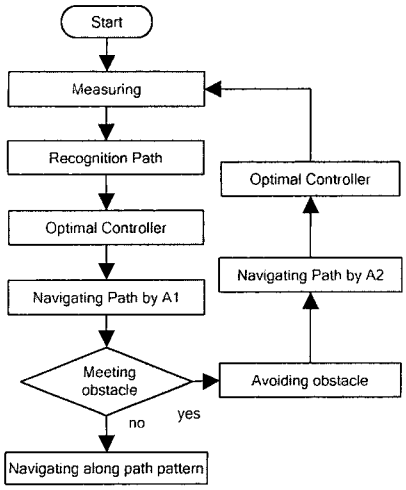

Fig. 5 Path generation algorithm

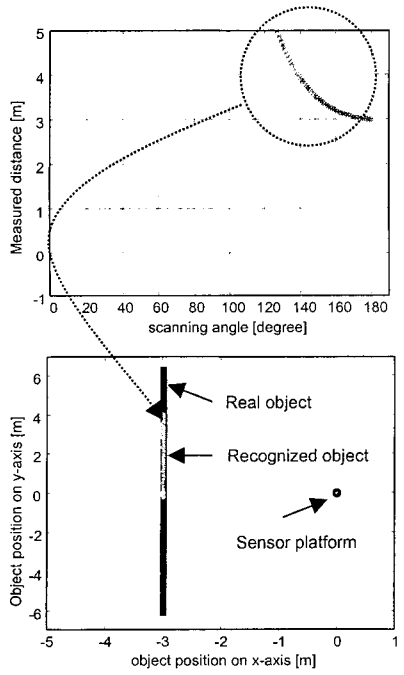

Fig. 6 One-side wall recognition

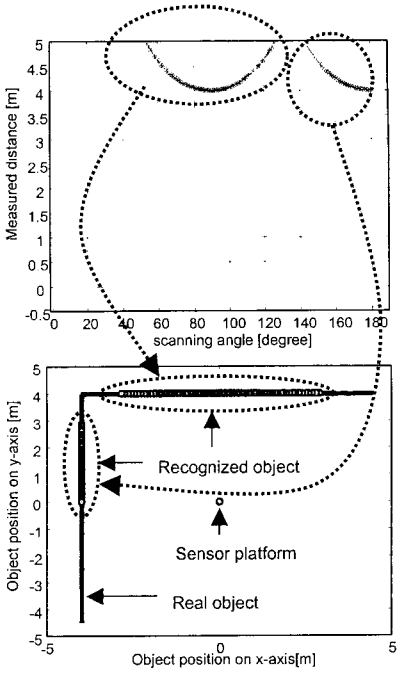

Fig. 7 Front and right side wall recognition

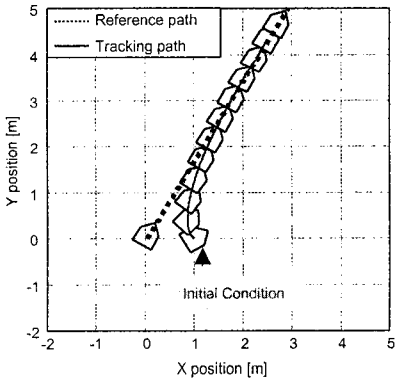

Fig. 8 Controlled model simulation when the initial conditions are $\tilde{\Psi}=-\pi/6$, $x=1$, $y=0$

controller based on the linearized model. The path generation is composed of the path recognition and path tracking and is simulated by applying the algorithm described in section 3.3

4.1 Path recognition

The initial results of the path recognition obtained by the AGV are shown in Fig. 6 and Fig. 7. The paths that can be driven by the AGV are modeled as combinations of lines. Figure 6 shows the case where a wall is detected on the right side of the AGV.

Figure 7 is the case where walls are detected on the front and right side of the AGV

4.2 Path tracking

The purpose of the controller is reference path tracking. The simulation results of the controlled

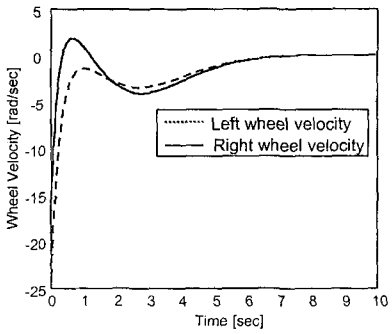

Fig. 9 Wheel velocities when initial condition is $\tilde{\Psi}=-\pi$, $x=1$, $y=0$

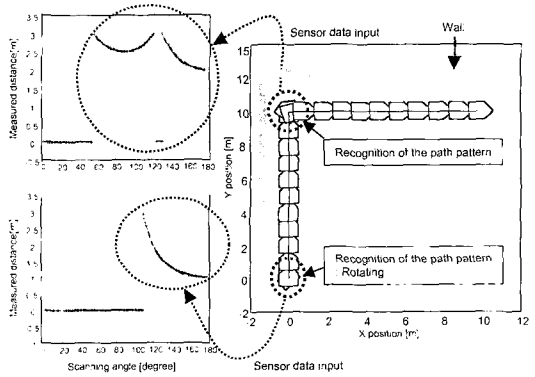

Fig. 10 Simulation for navigating the recognized path

AGV are shown in Fig. 8.

Figure 8 shows how the AGV tracks the reference path when the initial conditions are $x=1$, $y=0$, $\tilde{\Psi}=-\pi/6$.

The AGV will converge on the reference path with this control algorithm regardless of its location, position or direction. Figure 9 shows the angular velocity of the motor under these initial conditions.

4.3 Path generation

Initially, various operational environments are detected by using the sensor scanning method. First, a reference path is generated by using sensor data and then the AGV tracks it by applying the generated algorithm. Figure 10 shows the simulation result in which the AGV is navigating the recognized path pattern.

Figure 11 shows the generated navigation algorithm simulation of the AGV.

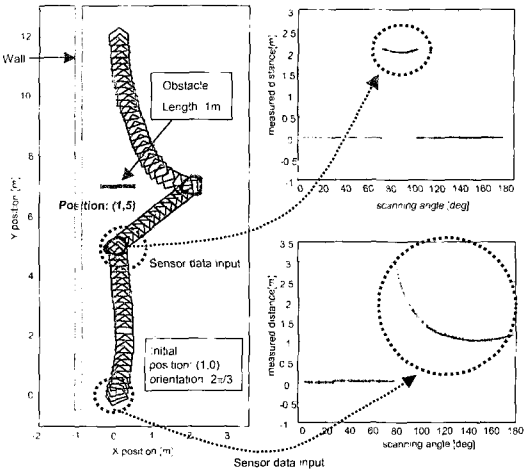

Fig. 11 Simulation of the navigation path algorithm

Figure 11 shows the AGV navigation based on path generation after recognition of the path pattern. It also shows the AGV tracking the reference path after avoiding an obstacle when the AGV has recognized the obstacle's size.

5. Experiments

Based on the results of the simulations, the path generation algorithm is applied to the AGV with the sensor platform mounted. The sensor data need to be inputted clearly. Consequently, experiments for path generation is performed based on the proposed algorithm.

5.1 Platform sensing

As the sensors are moving on the platform, sensor data can be quite noisy. An ultrasonic sensor which is rotating on the platform makes more noise than when motionless. A filtering method is required for reducing the noise. In this study, low and high pass filters are applied for clearing and reducing noise. Figure 12 shows the results of the filtered sensor data.

Compared with untreated sensor data, the noise level in the filtered data is remarkably lower. In order to determine the distance between the object and the monitoring sensor, the relationship between the voltage and the distance can be derived by using a linear interpolation method. With respect to linear interpolation, sensor outputs

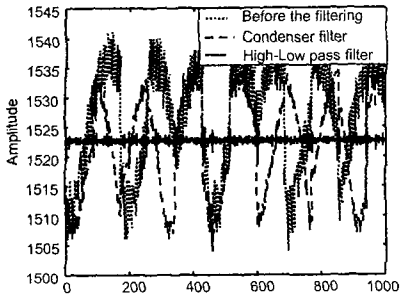

Fig. 12 The filtered sensor data

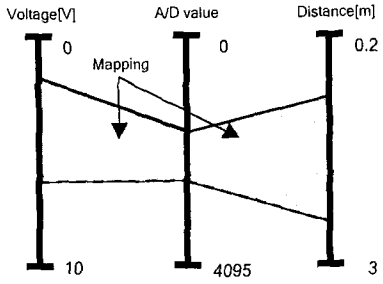

(a) Relationships of sensor input and recognition input

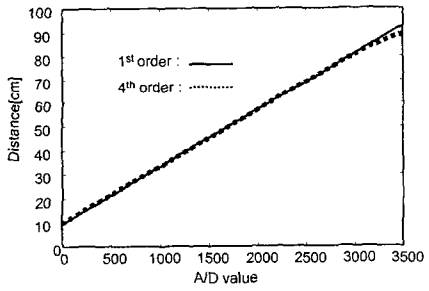

(b) Interpolation of sensor data

Fig. 13 Linear interpolation method for sensor data

were obtained for the distance range between 0. 2m and 3m in the increments of 5cm. The sensor outputs were interpolated using the average values. Figure 13 shows the linear interpolation method and the results. The sensor outputs were interpolated using the first or fourth order equations with the average values.

In the present study, the first and fourth order equation results were almost identical. After comparative evaluations, the first order interpolation equation was selected for reducing the calculation time.

5.2 AGV with platform

The control input is the angular velocity of the side wheels. In a real system, the angular velocity is transformed to 0~10 V and applied to the motor driver. Figure 14 shows the HYAV1 robot navigating with the proposed path generation algorithm.

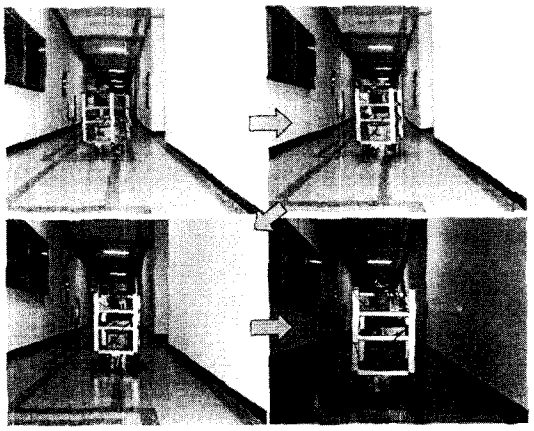

Fig. 14 Photos of the navigating AGV

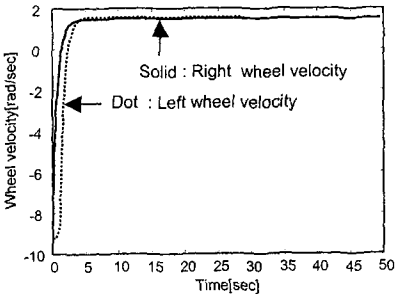

Fig. 15 Wheel velocities for the HYAV1 Experiment : The initial condition is $\tilde{\Psi}=-\pi/6$, $x=1$, $y=0$

In this experiment with 0.5 sec sampling time, the angular velocity was converged to the desired value in the simulation. The velocity command with discrete may increase the error at the final arrival point. This error may be ignored since it is insignificant compared with the navigation distance. Allowing for the limits of the motor angular velocity, the maximum velocity is set at 9. 23 [rad/sec].

Figure 15 shows the angular velocities of both wheels while tracking the reference path. As the results show, the wheel angular velocity is controlled so that the AGV can track the path. This experiment is a test for the path tracking ability of

the AGV when the orientation of the AGV is different from the reference path. In this experiment, control of the wheel was satisfactorily achieved under experimental conditions, but there were some errors. As the road surface is not perfectly flat, the error caused by the road surface can be regarded as unmodeled error between the road surface and the AGV's wheels. The error was measured as a distance between the final point after 40 sec and vertical distance from the HYAV1 center in navigation. A number of trials showed the average of the errors to be 0.52 m. The total average error was 0.66 m in the experiment. Considering the unmodeled error, the value of the experimental error may be regarded as 0.14 m. There are several causes for this error. The most significant cause is the friction and slip between the surface of the ground and the AGV wheels. The 2WD vehicle has the nonholonomic characteristic but this experiment shows that the controller is fairly good at path tracking.

6. Conclusions

In this paper, a navigation algorithm and a controller design for path generation of a 2WD AGV are proposed. A number of simulations and experiments involving real vehicle have demonstrated the validity of the proposed control algorithm. The results of the experiments show that the recognition of a path pattern can be constructed by the scanning method using the sensor platform. Path tracking is performed by the optimal controller based on a kinematic modeling. Path recognition is performed by the scanning method using only one sensor. The path generation algorithm was verified by the experiments.

The conclusions of this study are as follows:

(1) The kinematic model of the AGV is developed for controlling motors.

(2) The path pattern and the object magnitude were verified by the sensor platform utilizing only few sensors.

(3) The AGV tracks the generated path with the optimal controller.

(4) The scanning algorithm and optimal controller are validated(are validated) by applying them to a real AGV with sensor platform.

References

Aguilar, L. E., Hamel, T. and Soueres, P., 1997, "Robust Path Following Control for Wheeled Robots via Sliding Mode," *Proc. IROS 97 September* 7-11, pp. 1389~1395.

Division, C. B., 1984, "Ultrasonic Ranging System," Polaroid Corporation.

Flynn, A. M., 1988, "Combining Sonar and Infrared Sensors for Mobile Robot Navigation," *Int. Journal of Robotics Res.* Vol. 7, No. 6, pp. 5~14.

Hemami, A., Mehrabi, H. G. and Cheng, R. M. H., 1992, "Synthesis of an Optimal Control Law for Path tracking in Mobile Robots," *Automatica,* Vol. 28, pp. 383~387.

Henderson, T., 1987, *Workshop on Multi-Sensor and Infrared Sensors for Mobile Robot Navigation*, University of Utah Computer Science, Salt Lake City, UUCS-87~006.

Jang, J. H. and Han, C. S., 1997, "The State Sensitivity Analysis of the Front Wheel Steering Vehicle: In the Time Domain," *KSME International Journal*, Vol. 11, No. 6.

Kanayama, Y., Kimura, Y., Miyazaki, F. and Noguchi, T., 1991, "A Stable Tracking Control Method for an Nonholonomic Mobile Robot, IEEE/RSJ International Workshop on Intelligent Robots and Systems," pp. 1236~1241.

Kononov, O. A., Kirilchenko, A. A. and Yaroshevsky, V. S., 1993, "Laser Distance Measuring Systems for Mobile Robots," *Technology, Series FMS and Robototechnical Systems*, N1-2, pp. 39~44.

Laumond, J. P., 1993, "Controllability of a Multibody Mobile Robot," *IEEE Trans. On Robotics and Auto.*, Vol. 9, pp. 755~763.

Lee, T. C., Kai-Tai Song, K. T., Lee, C. H. and Teng, C. C., 1999, "Tracking Control of Mobile Robots Using Saturation Feedback Controller," *Proceedings of the 1999 IEEE Int. Conf. on Robotics and Auto.*, Detroit, Michigan, pp. 2639~2644.

Matthies, L. and Shafer, S. A., 1997, "Error

Modeling in Stereo Navigation," *IEEE Journal of Robotics And Automation*. Vol. RA-3, No. 3, pp. 239~248.

Miller, G. L. and Wagner, E. R., 1987, "An optical Rangefinder for Autonomous Robot Care Navigation," *Proceedings of the SPIE*, Vol. 851, Mobile Robots II, pp. 132~144.

Reister, D. B. and Pin, F. G., 1994, "Time -Optimal Trajectories for Mobile Robots With Two independent Driven Wheels," *Int. J. Robotics Research*, Vol. 13, pp. 38~54.

Park, K. C., Chung, H. Y., and Lee, J. G., 1999, "Point Stabilization of Mobile Robots Via State Space Exact Feedback Linearization," *Proceedings of the 1999 IEEE Int. Conf. on Robotics and Auto.*, Detroit, Michigan, pp. 2639 ~2644.

Park, T. J. and Han, C. H., 2000 "A Path Generation Algorithm of Autonomous Robot Vehicle By the Sensor Platform and Optimal Controller Based On the Kinematic Model," *15th KACC Int*, Korea.

Rosa, F. D. L., Najra, J. and Laugier, C., 1994, "Planning Robot Motion Strategies Under Geometric Constraints," *Proceedings of ICARCV'92*, pp. 1311~1315.

Samson, C. and Ait-Abderrahim, K., 1991. "Feedback Control of Nonholonomic Wheeled Cart in Catesian Space," *IEEE Int. Conf. on Robotics and Auto.*, pp. 1136~1141.

Yongji Wang, Linnett, J. A. and Roberts, J. W., 1996, "A Unified Approach to Inverse and Direct Kinematics for Four Kinds of Wheelded Mobile Robots and its Applications," *Proceedings of the 1996 IEEE Int. Conf. on Robotics and Auto.*, Minneapolis, Minnesota-April, pp. 3458~3465.

Yun, X. and Nilanjan Sarkar, 1996, "Dynamic Feedback Control of Vehicle with Two Steerable Wheels," *IEEE Inter. Con. on Robotics and Auto.*, pp. 3105~3110.

Zhao, Y. and Reyhanoglu, M., 1992, "Nonlinear Control of Wheeled Mobile Robots," *Proc. Of the 1992 IEEE/RSJ Inter. Con. on Intelligent Robots and Systems*, pp. 1967~1973.